The Astrophysical Journal Letters, 884:L37 (6pp), 2019 October 20 https://doi.org/10.3847/2041-8213/ab48f5

Puffy Accretion Disks: Sub-Eddington, Optically Thick, and Stable

Debora Lančová[1,2], David Abarca[3], Włodek Kluźniak[3], Maciek Wielgus[2,3,4], Aleksander Sądowski[5], Ramesh Narayan[2,4], Jan Schee[6], Gabriel Török[1], and Marek Abramowicz[1,2,3,7]
[1] Research Center for Computational Physics and Data Processing, Institute of Physics, Silesian University in Opava, Czech Republic; debora.lancova@fpf.slu.cz
[2] Black Hole Initiative at Harvard University, 20 Garden Street, Cambridge, MA 02138, USA; maciek.wielgus@gmail.com
[3] Nicolaus Copernicus Astronomical Centre, Polish Academy of Sciences, Bartycka 18, 00-716 Warsaw, Poland; wlodek@camk.edu.pl
[4] Center for Astrophysics, Harvard & Smithsonian, 60 Garden Street, Cambridge, MA 02138, USA
[5] Akuna Capital, 333 South Wabash Avenue, Chicago, IL 60604, USA
[6] Research Centre of Theoretical Physics and Astrophysics, Institute of Physics, Silesian University in Opava, Czech Republic
[7] Department of Physics, Göteborg University, Sweden
Received 2019 August 21; revised 2019 September 25; accepted 2019 September 28; published 2019 October 15

Abstract

We report on a new class of solutions of black hole accretion disks that we have found through three-dimensional, global, radiative magnetohydrodynamic simulations in general relativity. It combines features of the canonical thin, slim, and thick disk models but differs in crucial respects from each of them. We expect these new solutions to provide a more realistic description of black hole disks than the slim disk model. We are presenting a disk solution for a nonspinning black hole at a sub-Eddington mass accretion rate, $\dot{M} = 0.6\,\dot{M}_{\rm Edd}$. By the density scale-height measure the disk appears to be thin, having a high density core near the equatorial plane of height $h_\rho \sim 0.1\,r$, but most of the inflow occurs through a highly advective, turbulent, optically thick, Keplerian region that sandwiches the core and has a substantial geometrical thickness comparable to the radius, $H \sim r$. The accreting fluid is supported above the midplane in large part by the magnetic field, with the gas and radiation to magnetic pressure ratio $\beta \sim 1$, this makes the disk thermally stable, even though the radiation pressure strongly dominates over gas pressure. A significant part of the radiation emerging from the disk is captured by the black hole, so the disk is less luminous than a thin disk would be at the same accretion rate.

Unified Astronomy Thesaurus concepts: Accretion (14); Magnetohydrodynamical simulations (1966); General relativity (641); Radiative magnetohydrodynamics (2009); Black holes (162)

1. Introduction

The understanding of optically thick accretion disks has historically been strongly influenced by analytic models. Thus, one tends to think of thin disks, having in mind the geometrically thin α-disk model of Shakura & Sunyaev (1973), with the thickness to radius ratio $H/r \ll 1$; or of thick disks, having in mind the geometrically thick "Polish doughnuts" with $H/r > 1$ in the innermost parts, and a funnel through which most of the radiation is emerging (Jaroszyński et al. 1980); and of slim disks (Abramowicz et al. 1988) of thickness comparable to the circumferential radius, but usually smaller, $H < r$. In all cases the thickness H can be taken to be the vertical ($z \equiv r\cos\theta$) coordinate of the photosphere above the equatorial plane of symmetry, and for these three canonical models it happens to coincide also with the characteristic scale-height of density, h_ρ. A useful discriminant was thought to be given by the luminosity, L, of the disk in terms of the Eddington ratio $\lambda \equiv L/L_{\rm Edd}$, with $\lambda < 0.3$ thought to be appropriate for the thin disks, $0.3 < \lambda \lesssim 3$ for the slim disks, and $\lambda \gg 1$ for Polish doughnuts.

Spectral and flux observations of various black hole sources seem to be in agreement with the predictions of the three models in the stationary approximation. In particular, the multicolor spectrum expected from thin disks yielded good fits to observations of numerous accreting X-ray binaries (Mitsuda et al. 1984), and the XSPEC models of thin disk spectra, KERRBB and BHSPEC (Li et al. 2005; Davis et al. 2006), have been successfully used to fit numerous black hole disk spectra at low luminosities. Slim disks, physically differing from thin disks in allowing radial advection of the heat generated in viscous dissipation, predict somewhat different spectra (resulting from the temperature being proportional to the radius to the $-1/2$ power) and these were reported to fit both black hole X-ray binary sources of moderate peak luminosity, $\lambda \sim 0.6$ (Kubota & Makishima 2004; Straub et al. 2011) and ultraluminous X-ray sources (Vierdayanti et al. 2006; Caballero-Garcia et al. 2017). For an up-to-date review of modeling astrophysical sources by slim disks, see Czerny (2019).

While Polish doughnuts were amenable to numerical simulations early on (Igumenshchev & Abramowicz 2000), which supported the general picture of a bulbous disk terminating in a cusp, with a fairly narrow axial funnel trough which radiation could have escaped (had it been present in the simulations), the early numerical simulations had nothing to say about the structure of accretion disks at moderate and low accretion rates. Indeed, until recently, with their limited resolution and lack of radiative transport, numerical simulations of sub-Eddington optically thick accretion disks were simply assumed to correspond to the thin or slim disk models. Attention tended to focus on the mechanism of turbulent dissipation and angular momentum transport, as well as the generation and evolution of the internal magnetic field (Brandenburg et al. 1995; Machida & Matsumoto 2003).

Now that general relativistic magnetohydrodynamic (GRMHD) accretion-disk simulations have come of age and allow global simulations of geometrically thin disks, with (Ohsuga & Mineshige 2011; Mishra et al. 2016; Sądowski 2016; Fragile et al. 2018; Jiang & Blaes 2019) and without (Zhu & Stone 2018; Liska et al. 2019) radiation, it is time to revisit the theoretical properties of sub-Eddington accretion disks. We have simulated disks that are thermally stable in the regime where radiation

pressure dominates over gas pressure, and found that at moderate accretion rates they correspond to none of the three analytical models. Instead, in differing respects, they contain elements of each of the three classes of models. The density scale-height of our simulated disks corresponds to those of thin disk models, $h_\rho/r \ll 1$. However, the disks are advective, with the photon flux directed mostly inwards close to the inner edge of the disk, more in keeping with the expectations of slim disk models. The overall appearance is reminiscent of thick disks, with the radiation density highest in an axial funnel, with the height of the photosphere satisfying $H/r \sim 1$.

In this Letter we discuss a Schwarzschild metric simulation for a 10 solar mass black hole ($M = 10\,M_\odot$) with an accretion rate of $\dot{M} = 0.6\,\dot{M}_{\rm Edd}$, where we define $\dot{M}_{\rm Edd} = L_{\rm Edd}/(0.057c^2)$ with the usual Schwarzschild efficiency factor 0.057, and Eddington luminosity $L_{\rm Edd}$. We are using the gravitational radius, $M \equiv GM/c^2$, as the unit of length.

2. Puffy Disks

Simulating radiative thin disks, i.e., ones with low accretion rates, is numerically challenging in magnetohydrodynamics even when the disk is intrinsically stable (Sądowski 2016) because of the resolution requirements of the magnetorotational instability (MRI; Balbus & Hawley 1998). Additionally, radiation pressure dominated disks are known to be thermally unstable, with the Shakura & Sunyaev (1976) linear stability analysis prediction confirmed for α-viscosity disks in fully nonlinear, global, radiative, general relativistic, hydrodynamic simulations (Fragile et al. 2018). This instability has been shown to also hold when the turbulent dissipation is provided by MRI, both in shearing box simulations (Jiang et al. 2019) and in global simulations (Mishra et al. 2016).

It should not be a surprise, then, that radiative GRMHD simulations of accretion flows initialized with a radiation pressure dominated thin disk configuration ended in a rapid collapse of the disk to a state that was too thin for the MRI to be resolved (Mishra et al. 2016). Interestingly, even though most of the gas collapsed to a very thin disk, an optically thick atmosphere permeated by the radiation persisted like the grin of a Cheshire cat, with the photosphere remaining in its original position at a height of nearly $2\,M \gg h_\rho$. In other words, the degeneracy between the density scale height, h_ρ, and photospheric half thickness, H, of the disk was broken—they were no longer equal. However, as the simulation had to be terminated this could have been a transient phenomenon and remained but a tantalizing hint of what a "thin" disk may really look like. To date, there are no radiative GRMHD simulations of black hole disks at $\sim$0.1 to $0.3\dot{M}_{\rm Edd}$, so in fact we simply do not yet know what an MHD turbulent black hole disk should look like in theory, in the putative thin disk regime. Following our recent simulations, we are now in a position to describe the structure and appearance of stable $\sim 0.6\,\dot{M}_{\rm Edd}$ disks.

We have performed global, 3D, radiative GRMHD simulations of black hole disks at decreasing sub-Eddington accretion rates. To ensure thermal stability (Zheng et al. 2011) the disk was made to advect poloidal magnetic field with a significant radial component (Sądowski 2016) from the toroidal mass reservoir often included in disk simulations. Upon evolution of this field through the MRI a major component of the pressure is due to the magnetic field, with the plasma parameter $\beta = (p_{\rm gas} + p_{\rm rad})/p_{\rm mag} \sim 1$. Of the remaining components of pressure, radiation pressure (hugely) dominates over the gas pressure, and the opacity is dominated by electron scattering, in agreement with Shakura & Sunyaev (1973). The radiation field is evolved in the approximation of the M1 closure scheme (Levermore 1984; Sądowski et al. 2013). The simulations were performed with the KORAL code, and closely follow those of Sądowski (2016), which were performed for somewhat higher accretion rates. A detailed description of our simulations can be found in D. Lančová et al. (2020, in preparation). Here, we describe the striking features of the simulated stable, sub-Eddington, radiative accretion disks, illustrated by the $0.6\dot{M}_{\rm Edd}$ simulation results.

Figure 1 shows a meridional-plane snapshot of the density field (top left panel). It is evident that the accreting gas is concentrated toward the equator, the density scale height (defined as in Sądowski 2016) being $h_\rho \sim 0.1\,r$ (white dashed curve). In this sense the disk is geometrically thin. However the potentially observable surface of the disk, i.e., the photosphere (solid white line in all the figures) is at a much greater height, $H \approx r$, just like in a geometrically thick disk. This is not an academic distinction—clearly the shape and position of the photosphere will have significant consequences for the dependence of the flux observed at infinity as a function of the inclination angle to the observer (see Section 3), and for the inferred (so-called isotropic) luminosity of the source. Note that very little radiation is released at $r > 15\,M$, instead, much of it is advected to lower radii and then released into the funnel (bottom right panel of Figure 1).

The bottom left panel of Figure 1 shows that there is a great deal of turbulence in the disk, all the way up to the photosphere. Figure 2 shows that the disk is Keplerian, also (nearly) all the way up to the photosphere. This would not be surprising for the moderate mass accretion rate of $0.6\,\dot{M}_{\rm Edd}$, except that our disk is not geometrically thin, and the photosphere is at a height of $z = H \approx r$, so the region of Keplerian rotation is quite thick. Presumably the corotation is enforced by the turbulence.

As the above discussion makes clear, the cartoon separation of the matter in the vicinity of a black hole into a rotating and accreting disk and a quasistatic corona simply does not occur. Instead, the high density core of the disk is sandwiched by a fairly thick "puffy" layer of lower-density, magnetized, optically thick plasma participating in the overall flow, and a comoving atmosphere above the photosphere.

It is interesting to note that close to the equator there is a region of super-Keplerian rotation (below the black curve in Figure 2) extending from $r \approx 18\,M$ down to the ISCO (the innermost stable circular orbit), at $r = 6\,M$ for a nonspinning black hole. This is qualitatively similar to the expectations in a thick disk, which is sub-Keplerian at distances from the black hole larger than that of the center of the disk (pressure maximum), and super-Keplerian at smaller radii (Jaroszyński et al. 1980). By contrast, thin disks are slightly sub-Keplerian except close to the inner edge.[8]

The time-averaged quantities are shown in Figure 3. Note that the motion of the accreting fluid is not confined to the dense core within the scale-height h_ρ. Quite to the contrary, most of the inflow occurs above the core, and actually

[8] Specifically, in general relativity, thin disks become super-Keplerian close to the ISCO (Jaroszyński et al. 1980). In Newtonian gravity, α-disks are sub-Keplerian down to 1.4 r_+, where r_+ is the radius where the torque vanishes (Kluźniak & Kita 2000).

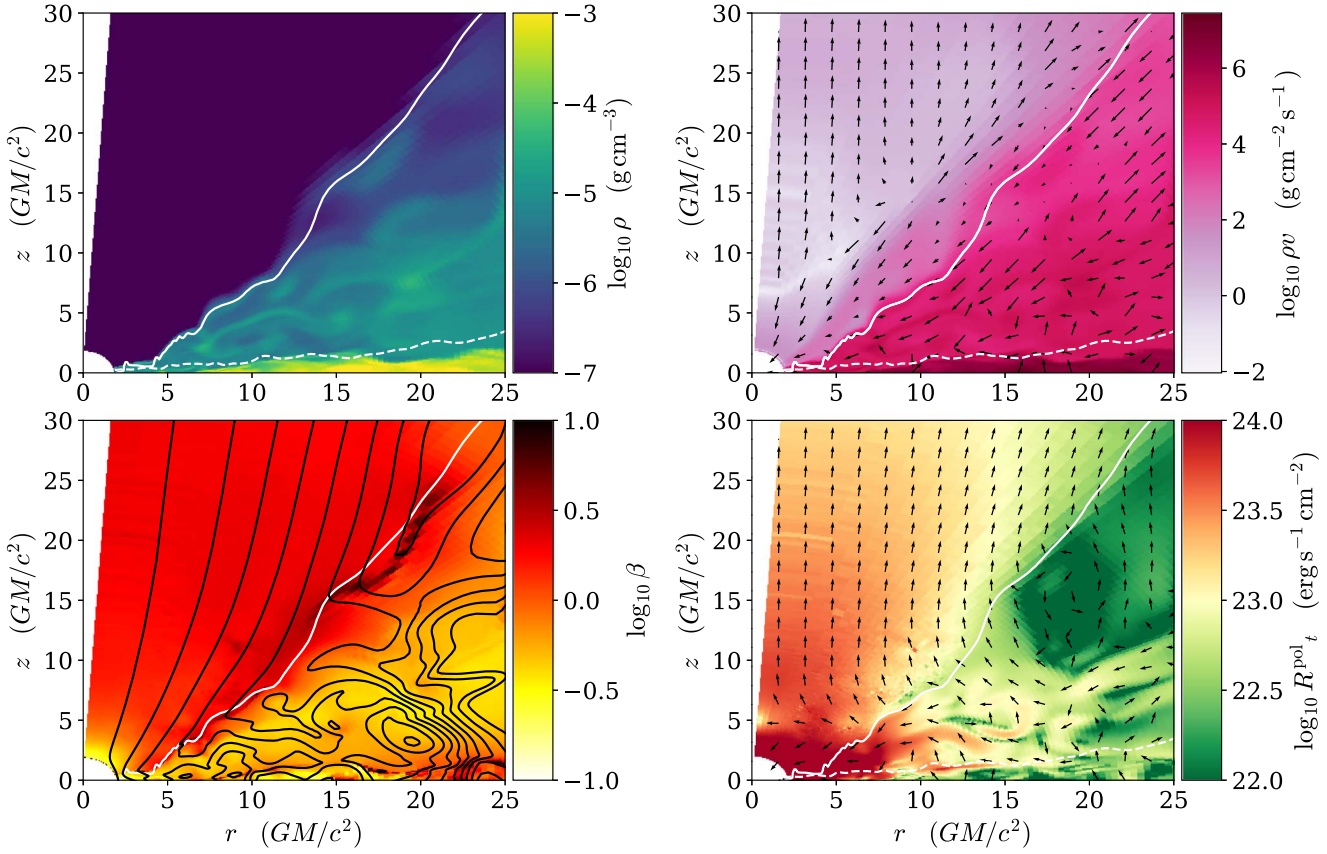

Figure 1. Snapshots showing various physical properties of the puffy disk with $\dot{M} = 0.6\dot{M}_{\mathrm{Edd}}$. The location of the photosphere is shown by the solid white line (the optical depth was computed along lines parallel to the z axis), the dashed white line shows the density scale-height, h_ρ. Upper left: gas density ρ. Upper right: gas momentum density ρv and vectors of gas velocity in the poloidal plane. Lower left: plasma parameter $\beta = (p_{\mathrm{rad}} + p_{\mathrm{gas}})/p_{\mathrm{mag}}$ (colors) with contours of the azimuthal component of the magnetic vector potential. Lower right: poloidal component of radiation flux $R_{\mathrm{t}}^{\mathrm{pol}}$ (color) and its direction (unit vectors).

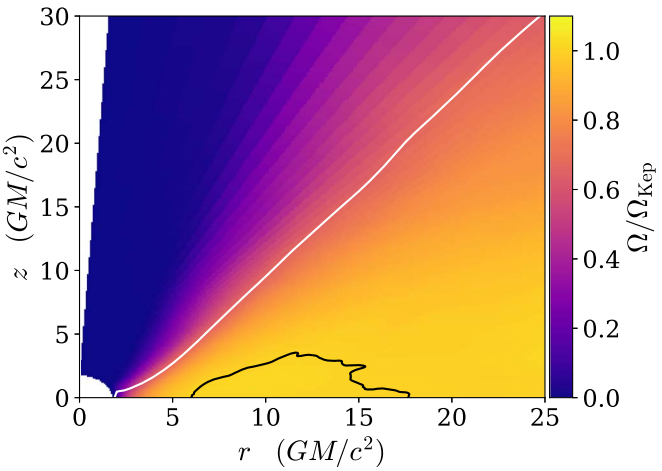

Figure 2. Angular velocity frequency Ω distribution scaled by the Keplerian value $\Omega_{\mathrm{Kep}} = (GM)^{1/2}R^{-3/2}$, where R is the cylindrical radius. Note that the fluid in the disk is Keplerian essentially all the way up to the photosphere. The black contour encloses the super-Keplerian region.

dominates it (Figure 4). The top right panel of Figure 3 shows a great deal of momentum inflow in the vicinity of the photosphere. For $r < 10M$ the fluid is moving toward the black hole in a region extending up to the stagnation surface (clearly visible as a whitish elongated area separating inwards and outwards pointing arrows), which is at least twice as high above the equatorial plane as the photosphere. Thus, there is no evidence for a Blandford & Payne (1982) launching of gas, even though the magnetic field lines are inclined outwards (bottom left panel of Figure 3) and the fluid is undergoing nearly Keplerian rotation (Figure 2). In the disk the magnetic field is dominated by its azimuthal component, while in the funnel it is dominated by its radial component. Thus, the field changes its character near the photosphere, which results in a minimum of magnetic pressure (p_{mag}) there.

It is also apparent (bottom right panel of Figure 3) that, contrary to what one assumes in the thin and slim disk models (which are one-dimensional, the equations being height-integrated), radiation that is about to leave the inner disk does not move vertically when still below the photosphere (solid white line), except at the largest radii. The radiation fluid inside the disk flows mostly radially inwards already at $r \approx 10\,M$, in contrast to the thin disk model in which the radiation flux vector rotates from the vertical to the radial direction only very close to the ISCO (Muchotrzeb & Paczyński 1982). In the language of slim disks, one would say that in the region defined by $z < 5\,M$ and $r < 10\,M$ most of the radiation is advected. Once radiation emerges through the photosphere at $r > 5\,M$, it escapes upward and slightly outwards through an optically thin funnel. There is an accompanying outflow of low-density plasma, apparently pushed out by the radiation. The radiation released in the inner disk at $z \leqslant 5\,M$ is lost in the black hole. As predicted by slim disk models, there is a great deal of advection of radiation within the disk. However, in the simulation the advection of radiation occurs also outside the

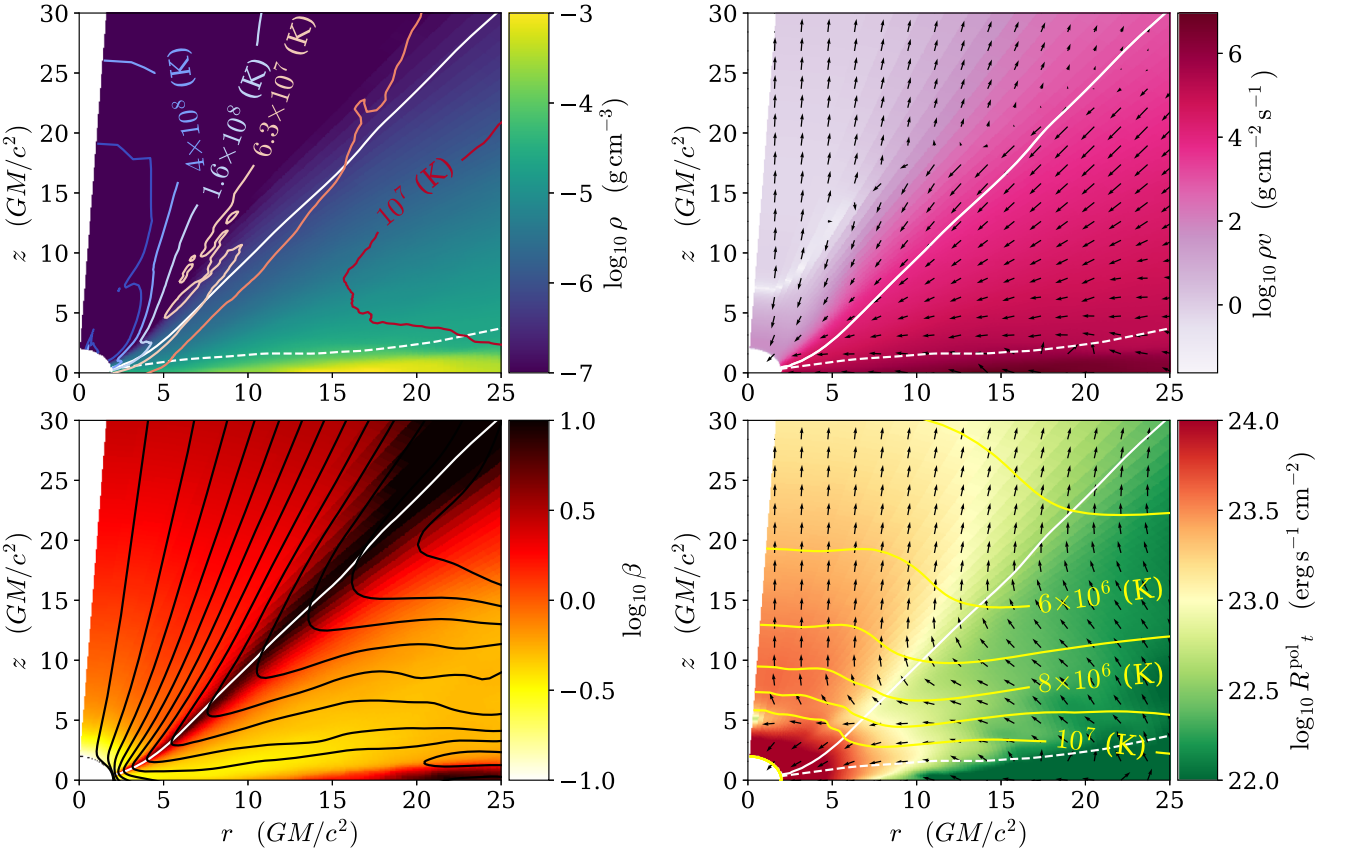

Figure 3. Time-averaged properties of the puffy disk with $\dot{M} = 0.6\dot{M}_{\rm Edd}$. The panels correspond to the panels in Figure 1, with additional information as follows. Upper left: contours of gas temperature, from left to right $T_{\rm gas} = 1.0 \times 10^9$, 4×10^8, 1.6×10^8, 6.3×10^7, 2.5×10^7, 1.0×10^7 K. Lower right: contours of radiation temperature, from top to bottom $T_{\rm rad} = 5.0$, 6.0, 7.0, 8.0, 9.0, 10.0 MK.

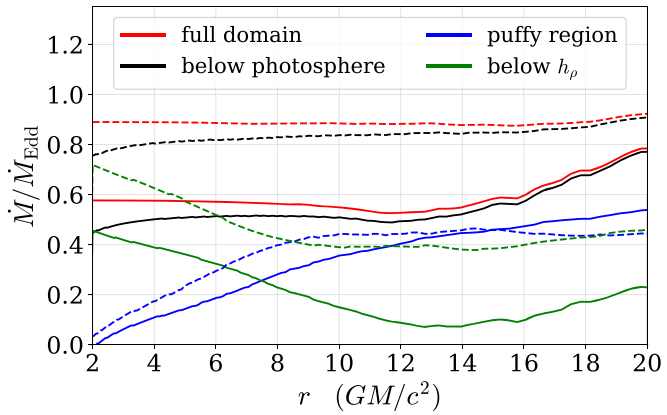

Figure 4. Mass accretion rate as a function of the radius. Dashed lines: Sądowski (2016). Solid lines: the current work. From top to bottom (at larger radii), red: integrated over the whole range of the polar angle; black: integrated under the photosphere; blue: integrated between the photosphere and the density scale-height h_ρ; green: integrated from the equatorial plane to the density scale-height h_ρ. At $r \gtrsim 8\,M$ most of the accretion occurs in the puffy region between the photosphere and the density scale-height surface h_ρ.

disk, with inflowing and outflowing radiation regions separated by a "photon stagnation surface," extending from the axis to the photosphere at $z \approx 5\,M$. For this reason the luminosity of the inner region[9] is $L = 0.36\,L_{\rm Edd}$, somewhat less than what one would have expected for a thin disk. However, most of this is emitted into a cone subtending much less than the full solid angle (Figure 5), so if observed close to the axis the inferred isotropic luminosity of the source would be significantly larger.

[9] Integrated between the z axis and the photosphere over a spherical surface segment of radius $r = 25\,M$.

3. Discussion

In our radiative GRMHD simulations we have found a new type of black hole accretion disk which may solve some long-standing problems of accretion-disk theory. First, for accretion rates relevant to the bright black hole sources the thin disk solution is known to be radiation pressure dominated in the innermost region, and it has been shown early on that such α-disks are disrupted by a viscous instability (Lightman & Eardley 1974), and are subject to a violent thermal instability (Pringle 1976; Shakura & Sunyaev 1976; Piran 1978); both these instabilities are also present in MRI simulations of radiation pressure dominated thin disks (Mishra et al. 2016). Our solutions are stabilized by magnetic pressure (Sądowski 2016), in line with the considerations of Zheng et al. (2011).

Both the thin disk and the slim disk models are based on height-integrated, azimuthally symmetric equations and so are intrinsically one-dimensional (1.5D). While slim disks are not subject to the thermal instability of thin disks, this property is not confirmed by simulations. In the absence of stabilizing magnetic field all global 3D radiative GR simulations of sub-Eddington disks in the radiation pressure dominated regime lead to disk collapse (Mishra et al. 2016; Sądowski 2016; Fragile et al. 2018). We surmise that the presence of advection alone is not enough to stabilize sub-Eddington disks. Furthermore, while capturing a great deal of the relevant

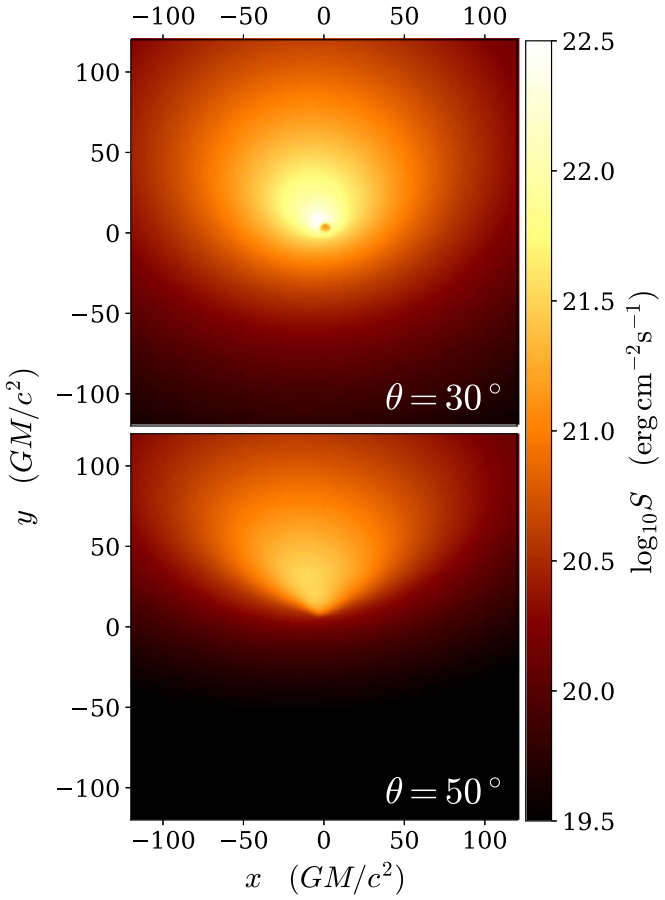

Figure 5. Ray-traced image of the inner part of the puffy disk for line-of-sight inclination θ of 30° and 50° to the axis.

physics, the thin and slim disk models, being intrinsically one-dimensional, do not allow for realistic meridional flow patterns, such as the equatorial backflows found for thin disks analytically (Urpin 1984; Kluźniak & Kita 2000), numerically (Regev & Gitelman 2002; Philippov & Rafikov 2017), and in hydrodynamic simulations of thick disks (Igumenshchev & Abramowicz 2000; Lee & Ramirez-Ruiz 2002). For the same reason they do not allow for nontrivial patterns in the flow of radiation, such as those observed in our 3D simulations (bottom right panels of Figures 1 and 3).

From the observational side, studies of AGNs have recognized the need for "elevated" disks, thicker than the standard thin disk solutions (Begelman & Silk 2017). Our models respond to this need and correspond to the recent magnetized disk models of Mishra et al. (2019). The latter work, a Newtonian simulation without radiation, has superior resolution and shows a spiral pattern of accretion, which has not been obtained in our limited azimuthal domain (see the Appendix). Our findings of accretion predominantly occurring above the high density core agree with those of Zhu & Stone (2018) and Mishra et al. (2019). In fact, for the first time in an MRI simulation, Mishra et al. (2019) find an equatorial backflow, their meridional accretion flow pattern being reminiscent of the analytic α-disk results of Kluźniak & Kita (2000). We do not find clear evidence of such backflow in our simulation, it would be interesting to check whether its absence is a result of the strong radiation field or strong gravity.

We also expect puffy disk spectra to be different from those of the slim disks (for instance, small density and high temperature imply a large color correction to the thermal spectrum) and to this end we will be post-processing our simulation to compute the spectra at infinity (D. Lančová et al. 2020, in preparation). The computed appearance at infinity of the puffy disk (Figure 5) differs from the usual image of a warped thin disk with a hole in it. At small and moderate inclinations (up to about 40° away from the axis) a wide bright funnel is clearly apparent with a darker spot just above the black hole (which itself is partially obscured by the hot gas). At larger inclinations, the near side and the bottom of the funnel are shadowed by the optically thick disk.

The $0.6\,\dot{M}_{\rm Edd}$ accretion rate in the reported simulation may correspond, close to the peak of their brightness, to such black hole sources as LMC X-3, for which an XSPEC model of slim disk spectra was developed (SLIMBB, Straub et al. 2011), a model which may now need to be supplanted.[10]

The puffy disk is expected to have different timing properties than the thin disk and its oscillation eigenmodes may differ from those of diskoseismology (Wagoner 1999; Kato 2001) and of accretion tori (Rezzolla et al. 2003; Blaes et al. 2006; Mazur et al. 2016; Mishra et al. 2017). This may be relevant to the theory of black hole quasi-periodic oscillations (Remillard & McClintock 2006). The phenomenology of state transitions in black hole X-ray binaries may also need reinterpretation.

The authors thank Andrew Chael and Brandon Curd for support with the KORAL code. The computations in this work were supported by the PLGRID INFRASTRUCTURE through which access to the Prometheus supercomputer, located at ACK Cyfronet AGH in Kraków, was provided. This work was supported in part by the Polish NCN grant 2013/08/A/ST9/00795, the INTER-EXCELLENCE project No. LTI17018 aimed to strengthen international collaboration of Czech scientific institutions, and the Black Hole Initiative at Harvard University, which is funded by grants the John Templeton Foundation and the Gordon and Betty Moore Foundation to Harvard University. M.A. acknowledges the Polish NCN grant 2015/19/B/ST9/01099, M.A., D.L., and G.T. the Czech Science Foundation grant No. 17-16287S, and D.L. the student grants SGS/13/2019 and MSK/03788/2017/RRC.

Appendix

Here, we provide some details of the numerical simulations. The essential technical description of the KORAL code is given in Sądowski et al. (2013, 2014). We extended the $\sim 0.8\dot{M}_{\rm Edd}$ results published in Sądowski (2016) to obtain a family of stable solutions at lower accretion rates. In our current work we only use reservoirs of mass with quadrupole topology of the magnetic field, resulting in strongly magnetized stable solutions. Initially, the toroidal reservoir extends from $r = 42\,M$ to $r = 500\,M$. For initial conditions of disks with successively lower accretion rates we are using the results of a previous simulation at larger $\dot{M}$, scaling down the gas density, internal energy, radiation energy density, and magnetic field by a constant factor. This preserves temperature, the gas to magnetic pressure ratio, and β.

The $0.6\dot{M}_{\rm Edd}$ simulation has achieved inflow equilibrium out to $r \approx 20\,M$ in a run of duration $t = 15000\,GM/c^3$.

[10] Several other slim-disk spectral fitting routines are available, e.g., SLIMULX (Caballero-Garcia et al. 2017), and others at https://heasarc.nasa.gov/xanadu/xspec/models/slimdisk.html (based on Kawaguchi 2003), and in the GitLab project https://projects.asu.cas.cz/bursa/slimbh/tree/master.

Throughout the domain we are using horizon-penetrating, modified Kerr-Schild coordinates. The simulations demand an enormous amount of computational time even with a very effectively configured grid, strongly concentrated around the equatorial plane, so we use only a $\pi/2$ wedge with periodic boundary conditions in the azimuthal direction. It has been shown by Sądowski (2016) that in the disk properties that we discuss in this Letter there is no significant difference between 3D simulations over a $\pi/2$ wedge and a domain spanning the full 2π azimuthal angle. The resolution of the grid ($N_r \times N_\theta \times N_\phi$) is $320 \times 320 \times 32$, which is sufficient to resolve the MRI (Balbus & Hawley 1998) with quality factors $\langle Q_\theta \rangle \approx 25$ and $\langle Q_\phi \rangle \approx 20$ in the accretion flow.

The inner disk ($r < 25\,M$) simulation output (temperature, density, velocity, and magnetic field), and its extrapolation for $25\,M \leqslant r < 500\,M$, was postprocessed to generate the ray-traced images of the disk (Figure 5). To this end, the radiation field was solved for with the HEROIC code (Zhu et al. 2015; Narayan et al. 2016), including bremsstrahlung, synchrotron, and Comptonization processes.

ORCID iDs

Debora Lančová https://orcid.org/0000-0003-0826-9787
Maciek Wielgus https://orcid.org/0000-0002-8635-4242
Gabriel Török https://orcid.org/0000-0003-3958-9441

References

Abramowicz, M., Jaroszyński, M., & Sikora, M. 1978, A&A, 63, 221
Abramowicz, M. A., Czerny, B., Lasota, J.-P., & Szuszkiewicz, E. 1988, ApJ, 332, 646
Balbus, S. A., & Hawley, J. F. 1998, RvMP, 70, 1
Begelman, M. C., & Silk, J. 2017, MNRAS, 464, 2311
Blaes, O. M., Arras, P., & Fragile, P. C. 2006, MNRAS, 369, 1235
Blandford, R. D., & Payne, D. G. 1982, MNRAS, 199, 883
Brandenburg, A., Nordlund, A., Stein, R. F., & Torkelsson, U. 1995, ApJ, 446, 741
Caballero-Garcia, M. D., Bursa, M., Dovčiak, M., et al. 2017, CoSka, 47, 84
Czerny, B. 2019, Univ, 5, 131
Davis, S. W., Done, C., & Blaes, O. M. 2006, ApJ, 647, 525
Fragile, P. C., Etheridge, S. M., Anninos, P., Mishra, B., & Kluźniak, W. 2018, ApJ, 857, 1
Igumenshchev, I. V., & Abramowicz, M. A. 2000, ApJS, 130, 463
Jaroszyński, M., Abramowicz, M. A., & Paczyński, B. 1980, AcA, 30, 1
Jiang, Yan-Fei, Blaes, O., Stone, J. M., & Davis, S. W. 2019, arXiv:1904.01674
Jiang, Y.-F., Stone, J. M., & Davis, S. W. 2019, ApJ, 880, 67
Kato, S. 2001, PASJ, 53, 1
Kawaguchi, T. 2003, ApJ, 593, 69
Kluźniak, W., & Kita, D. 2000, arXiv:astro-ph/0006266
Kubota, A., & Makishima, K. 2004, ApJ, 601, 428
Lee, W. H., & Ramirez-Ruiz, E. 2002, ApJ, 577, 893
Levermore, C. D. 1984, JQSRT, 31, 149
Li, L., Zimmerman, E. R., Narayan, R., & McClintock, J. E. 2005, ApJS, 157, 335
Lightman, A. P., & Eardley, D. M. 1974, ApJL, 187, L1
Liska, M., Tchekhovskoy, A., Ingram, A., & van der Klis, M. 2019, MNRAS, 487, 550
Machida, M., & Matsumoto, R. 2003, ApJ, 585, 429
Mazur, G. P., Zanotti, O., Sądowski, A., Mishra, B., & Kluźniak, W. 2016, MNRAS, 456, 3245
Mishra, B., Begelman, M. C., Armitage, P. J., & Simon, J. B. 2019, arXiv:1907.08995
Mishra, B., Fragile, P. C., Johnson, L. C., & Kluźniak, W. 2016, MNRAS, 463, 3437
Mishra, B., Vincent, F. H., Manousakis, A., et al. 2017, MNRAS, 467, 4036
Mitsuda, K., Inoue, H., Koyama, K., et al. 1984, PASJ, 36, 741
Muchotrzeb, B., & Paczyński, B. 1982, AcA, 32, 1
Narayan, R., Zhu, Y., Psaltis, D., & Sądowski, A. 2016, MNRAS, 457, 608
Ohsuga, K., & Mineshige, S. 2011, ApJ, 736, 2
Philippov, A. A., & Rafikov, R. R. 2017, ApJ, 837, 101
Piran, T. 1978, ApJ, 221, 652
Pringle, J. E. 1976, MNRAS, 177, 65
Regev, O., & Gitelman, L. 2002, A&A, 396, 623
Remillard, R. A., & McClintock, J. E. 2006, ARA&A, 44, 49
Rezzolla, L., Yoshida, S., & Zanotti, O. 2003, MNRAS, 344, 978
Sądowski, A 2016, MNRAS, 459, 4397
Sądowski, A., Narayan, R., McKinney, J. C., & Tchekhovskoy, A 2014, MNRAS, 439, 503
Sądowski, A., Narayan, R., Tchekhovskoy, A., & Zhu, Y. 2013, MNRAS, 429, 3533
Shakura, N. I., & Sunyaev, R. A. 1973, A&A, 24, 337
Shakura, N. I., & Sunyaev, R. A. 1976, MNRAS, 175, 613
Straub, O., Bursa, M., Sądowski, A., et al. 2011, A&A, 533, A67
Urpin, V. A. 1984, SvA, 28, 50
Vierdayanti, K., Mineshige, S., Ebisawa, K., & Kawaguchi, T. 2006, PASJ, 58, 915
Wagoner, R. V. 1999, PhR, 311, 259
Zheng, S.-M., Yuan, F., Gu, W.-M., & Lu, J.-F. 2011, ApJ, 732, 52
Zhu, Y., Narayan, R., Sądowski, A., & Psaltis, D. 2015, MNRAS, 451, 1661
Zhu, Z., & Stone, J. M. 2018, ApJ, 857, 34